Temperature Dependence of Ion Permeation at the Endplate Channel

HELENE M. HOFFMANN and VINCENT E. DIONNE

From the Department of Medicine, Division of Pharmacology, University of California at San Diego, La Jolla, California 92093

ABSTRACT The dependence of acetylcholine receptor mean single-channel conductance on temperature was studied at garter snake twitch-muscle endplates using fluctuation analysis. In normal saline under conditions where most of the endplate current was carried by Na^+, the channel conductance increased continuously from near 0°C to ~23°C with a Q_{10} of 1.97 ± 0.14 (mean ± SD). When 50% of the bath Na^+ was replaced by either Li^+, Rb^+, or Cs^+, the Q_{10} did not change significantly; however, at any temperature the channel conductance was greatest in Cs-saline and decreased with the ion sequence Cs > Rb > Na > Li. The results were fit by an Eyring-type model consisting of one free-energy well on the extracellular side of a single energy barrier. Ion selectivity appeared to result from ion-specific differences in the well and not in the barrier of this model. With a constant barrier enthalpy for different ions, well free-energy depth was greatest for Cs^+ and graded identical to the permeability sequence. The correlation between increased well depth (i.e., ion binding) and increased channel conductance can be accounted for by the Boltzmann distribution of thermal energy.

INTRODUCTION

The nicotinic acetylcholine receptor is the prototypical example of a chemically activated membrane channel. The functional entity includes two binding sites for agonist molecules and a gated, cation-selective channel. Located in great numbers postjunctionally at nicotinic cholinergic synapses, the receptor binds nerve-released acetylcholine and responds by briefly opening its ion channel. Small cations pass through the open channel to cause a localized depolarization of the postjunctional membrane.

The open acetylcholine receptor (AChR) channel is relatively nonselective, relying upon ion size, aqueous mobility, and charge as the main factors that determine permeability (Huang et al., 1978; Gage and Van Helden, 1979; Adams et al., 1980). However, several experimental observations indicate that permeant ions interact weakly with the channel and appear to bind to it during the translocation process (Lewis, 1979; Lewis and Stevens, 1979;

Address reprint requests to Dr. Vincent E. Dionne, Division of Pharmacology, M-013H, University of California at San Diego, La Jolla, CA 92093.

J. GEN. PHYSIOL. © The Rockefeller University Press · 0022-1295/83/05/0687/17 $1.00 687
Volume 81 May 1983 687-703

Marchias and Marty, 1979; Adams et al., 1981). If ions do bind at some point as they pass through the channel, it must be that they escape by acquiring small amounts of thermal energy. On this basis one would expect that the macroscopic single-channel conductance, γ, would exhibit some degree of temperature dependence. However, in several reports on chemically activated channels, there has been little uniformity of agreement. Anderson and Stevens (1973) reported no temperature dependence of γ in AChR channels of frog muscle. However, using *m. omohyoideus* from mouse, Dreyer et al. (1976) reported that γ changed suddenly about twofold near 25°C. Fischbach and Lass (1978) and Lass and Fischbach (1976) reported a continuous although nonlinear Arrhenius plot for γ in cultured chick muscle, which was similar to that obtained by Anderson et al. (1977) in glutamate-activated channels of locust muscle. Other experiments on AChR channels have found temperature dependence that was monotonic over the range examined; Gage and Van Helden (1979) obtained a Q_{10} of 1.0 at toad neuromuscular junction, whereas Sachs and Lecar (1977) reported 1.7 and Nelson and Sachs (1979) reported 1.3 in cultured chick skeletal muscle.

In view of these diverse reports we have sought to understand the energetics of ion permeation by examining the temperature dependence of single-channel conductance in AChR channels of garter snake neuromuscular junctions. We used this preparation because (*a*) it was well suited to microelectrode techniques and (*b*) a considerable amount of information was available on the receptor response (Burden et al., 1975; Hartzell et al., 1975; Kuffler and Yoshikami, 1975; Dionne and Parsons, 1981; Dionne and Leibowitz, 1982). Single-channel conductance was measured using fluctuation analysis in cells bathed in solutions containing different alkali metal cations. As temperature was increased, mean single-channel conductance increased monotonically with an average Q_{10} of 1.95; conductance at any temperature was graded Cs > Rb > Na > Li. The results were fit with an Eyring-type model consisting of an energy barrier with one relatively shallow well on its extracellular side. The transfer enthalpy over the barrier was the same for the four cations tested; however, the well depth was inversely correlated with conductance. That is, as the apparent binding affinity between ion and channel increased, the mean single-channel conductance for that ionic species also increased. This paradox can be explained by the Boltzmann distribution of thermal free energy.

METHODS

Garter snakes (*Thamnophis*) were obtained from Carolina Biological Supply Co., Burlington, NC. They were killed by decapitation, and whole costocutaneous muscles, including a portion of the rib and scale into which they inserted, were removed. Excised muscles were mounted in a glass-bottomed lucite chamber and bathed in one of several salt solutions. Nomarski optics were used to identify single endplates on twitch-muscle fibers.

Four different saline bathing solutions were used in this study. The normal physiological salt solution had the following composition (mM): 159 NaCl, 2.15 KCl, 1.0 $CaCl_2$, 4.2 $MgCl_2$, 1.0 HEPES, pH 7.2. Three other solutions were prepared by equimolar substitution of 50% of the Na in the normal solution with Li^+, Rb^+, or Cs^+. Mean single-channel cord conductance was estimated by fitting a single Lorentzian

curve to averaged difference spectra of ACh-induced noise. For a description of these standard techniques the reader should refer to Anderson and Stevens (1973), Dionne and Parsons (1981), and Dionne (1981). Noise data were bandpass-filtered between 2 Hz and either 500 or 1,000 Hz before digital sampling. Although it would have been preferable to make these measurements in solutions where 100% of the Na had been replaced by the ion of interest, that was not possible. In such solutions the rate of spontaneous miniature endplate currents was so high that no useful noise could be collected for the estimate of γ. Although the use of 50%-substituted solutions complicated the data analysis, it made the study feasible without resorting to less physiological measures.

The endplate region on twitch-muscle fibers was voltage-clamped with two 3 M KCl-filled microelectrodes, and endplate currents were induced by iontophoretic application of ACh. Details of these methods can be found in Dionne and Parsons (1981).

Temperature was adjusted by cooling the recording chamber with two Peltier thermoelectric devices (Cambridge Thermionic Corp., Cambridge, MA) or by circulating heated water through a metal plate beneath the chamber. The temperature was measured with a small, Teflon-covered thermocouple positioned in the saline bath within several millimeters of the recording microelectrodes. Although the temperature was not uniform throughout the test bath, the temperature gradient between the recording site and the thermocouple was negligible.

RESULTS

Measurements of single-channel conductance were made in normal saline and in salines where 50% of the Na^+ was replaced by equimolar amounts of Cs^+, Rb^+, or Li^+. For the measurements presented here, the membrane potential was held at voltages between -79 and -106 mV, a range that brackets the expected Nernst potential for K^+ in these cells. Under these conditions, the net endplate current flowing in any one AChR channel will be dominated by the inward flux component, so that the temperature-dependent changes in γ reported here should reflect changes in the inward flux of the alkali metal cations in the bath.

In normal Na^+ saline, γ increased about fourfold as the temperature was raised from near 0 to 22°C. This change is illustrated in Fig. 1, where both the results from a single cell and the compiled results of 43 measurements on 12 cells are presented. The temperature dependence was estimated using a linear least-squares regression. The slope of the line fitted to the compiled data in Fig. 1B was $-5{,}239 \pm 519$°K, which corresponds to a Q_{10} of 1.97 ± 0.14 (mean ± SD).

In the 50%-substituted salines containing Cs^+, Rb^+, or Li^+, similar increases in γ were observed as the temperature increased. The compiled data for each case are shown in Fig. 2 and the slopes of the Arrhenius plots are given in Table I.

As reported for other preparations (Ascher et al., 1978; Gage and Van Helden, 1979), single-channel conductance also depended upon the permeant ionic species. This is evident from comparison of the data in Figs. 1 and 2 at any temperature. The mean single-channel conductance in the different 50%-substituted salines at 10°C appears in Table I.

These data have been described as if they were the result of a direct effect

of temperature upon ion permeation. Before making this conclusion, two other sources of temperature dependence were considered and eliminated by experiment. First, temperature might affect the ion selectivity of the AChR channel and so produce an apparent change in γ. However, the relative permeabilities of the four cations studied did not change with temperature, and the endplate current reversal potential, V_R, measured in a representative sample of cells in each solution, appeared to be temperature independent. The reversal potential data for normal Na saline are shown in Fig. 3; $V_R = -5.60 \pm 2.09$ mV (mean ± SD), 70 measurements between 1.8 and 26.6°C. A similar insensitivity of V_R on temperature was observed in the 50%-substituted salines (Li:Na, −5.3

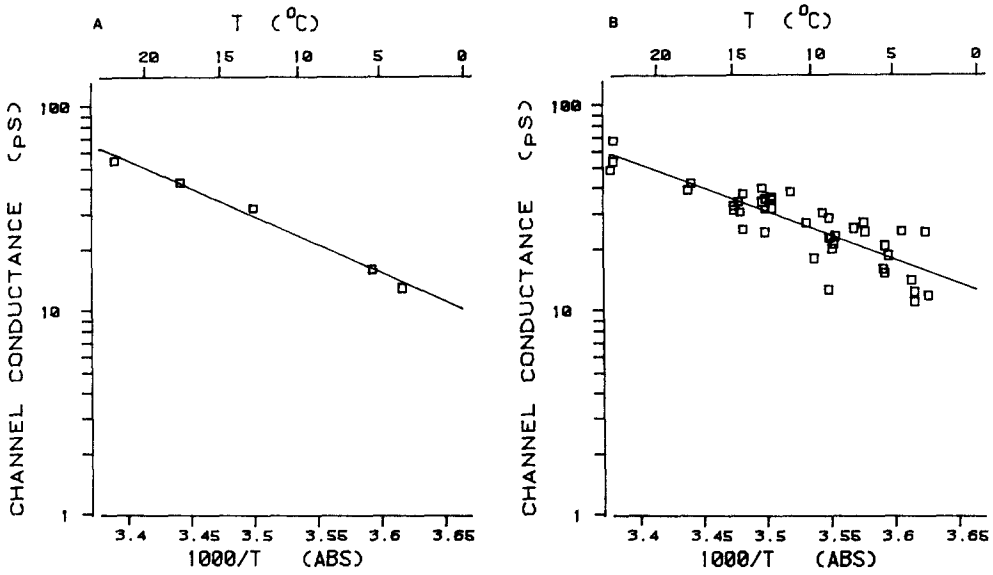

FIGURE 1. Temperature dependence of single-channel conductance in normal saline. Mean single-channel conductance (pS) was plotted against the reciprocal of absolute temperature (°K) and fitted by linear regression. (A) Five values were recorded from one cell at −80 mV between 3.6 and 22.0°C; slope = −6,441 ± 415°K (mean ± SD). (B) 43 values from 12 cells are plotted; slope = −5,239 ± 519°K. Further details are in the text.

± 2.9; Cs:Na, −4.7 ± 2.7). If a temperature-induced change in V_R were the source of our results, a shift of ~65 mV should have occurred over the temperature range studied. Second, AChR channels might close through a variety of mechanisms, with temperature altering whichever mechanism was expressed. This could produce an apparent change in conductance. In this case, the simple kinetic model on which our estimates of γ are based would not be applicable at all temperatures. We would expect the endplate current spectra to exhibit multiple components that shifted as temperature was changed. However, this was not observed. Spectra were always well described by a single Lorentzian component (Fig. 4).

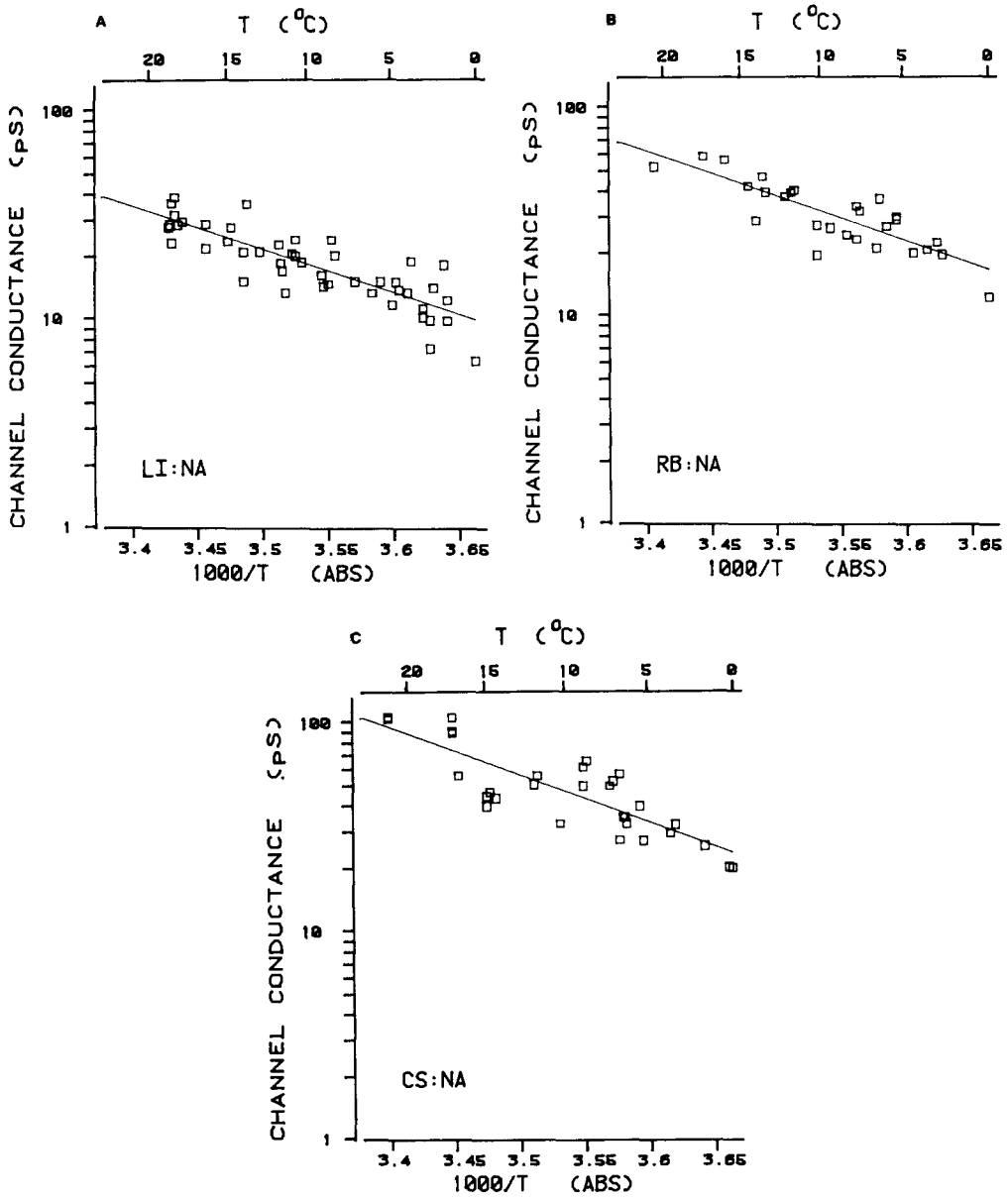

FIGURE 2. Temperature dependence of single-channel conductance in 50%-substituted salines. (A) Li was substituted. 46 values from 21 cells were recorded at voltages between −79 and −93 mV; slope = −4,892 ± 453°K. (B) Rb was substituted. 27 values from 17 cells were recorded at voltages between −79 and −91 mV; slope = −5,120 ± 657°K. (C) Cs was substituted. 30 values from 19 cells were recorded between −79 and −100 mV; slope = −5,377 ± 663°K. Notice that at any temperature the mean conductance is greatest for Cs and decreases as Cs:Rb:Na:Li.

QUANTITATIVE DESCRIPTION AND DISCUSSION

These data contain two separate kinds of information about the energetics of ion permeation: (*a*) the temperature dependence of mean single-channel conductance, and (*b*) the ion dependence of conductance magnitude. By modeling these results, we hoped to obtain some insight into the mechanism of ion permeation. We chose the Eyring formalism for model-building because of its computational tractability and for the relatively simple conceptual framework it offered. In general, we sought the least complex well-barrier model that was consistent both with our data and that of others. Below we will show that the simplest model with just one barrier cannot account for all the data in a consistent manner, but that a model incorporating a barrier together with at least one binding site is needed.

Both the single-barrier (1B) and the one-barrier/one-site (1B1S) models (see

TABLE I
SUMMARY OF MEASUREMENTS

Solution	*N*	Slope	γ at 10°C	γ/γ_{Na} at 10°C
		°*K*	*pS*	
Li-Na	46	−4,892±453	18.1±0.6	0.70±0.03
Na	43	−5,239±519	25.7±0.8	1.00±0.05
Rb-Na	27	−5,120±657	30.8±1.2	1.20±0.06
Cs-Na	30	−5,377±663	45.6±2.5	1.77±0.11

These data summarize the measurements in the four test solutions. The solutions are identified according to the major current-carrying ions. *N* is the number of measurements. The Arrhenius plot slope is given as the mean ± SD; the average conductance at 10°C and the conductance ratios are tabulated as means ± SE. The average conductance at 10°C was evaluated from the compiled data plotted in Figs. 1 and 2 using the fitted lines.

Figs. 5A and 6A) were developed in a manner similar to that used by Lewis (1979) and Lewis and Stevens (1979). The models did not specifically include ion competition for passage through the channels (see below). The general approach was to express the net ionic flux through the open channel as the difference between two one-way flux terms, each described by the thermodynamic parameters of the barrier model with Eyring rate theory. The expression for the net flux was then simplified by rewriting it as a sum of separate terms for each of the permeant cations and dropping terms made small by the specific measurement conditions. More precisely, since the measurements were collected at membrane voltages near the K^+ Nernst potential, the net K^+ flux was neglected. Furthermore, we assumed the flux of foreign cations would be inward-directed only. We also assumed that the intracellular Na^+ concentration did not change significantly during our measurements; thus, the outward Na^+ flux was neglected because it should always be <0.5% of the inward Na^+ component. Finally, we neglected the small contributions of the minority cations (Ca^{2+}, Mg^{2+}) to the net flux. The result expressed the net ionic flux as the sum of the inward-directed fluxes of Na^+ and one foreign cation X^+ when

it was present. For the 1B model this expression is

$$i_{net} = F\nu[Na^+]\exp\left(-\frac{\Delta U_O + F\delta V}{RT}\right) + F\nu[X^+]\exp\left(-\frac{\Delta U_X + F\delta V}{RT}\right). \quad (1)$$

Here the flux units are coulombs per second, F is the Faraday, V is the membrane voltage, R is the gas constant, ν is the vibration frequency, T is the absolute temperature, and δ is the fractional distance through the transmembrane electric field at which the barrier peak exists. The terms ΔU_O and ΔU_X give the free energies of the barrier peak relative to the solution levels for Na^+ (subscript O) and the foreign cation X^+. The ion concentrations are those for the bath. We divided this net flux term by the apparent driving potential, $V - V_R$, to express the macroscopic single-channel cord conductance, γ. In the

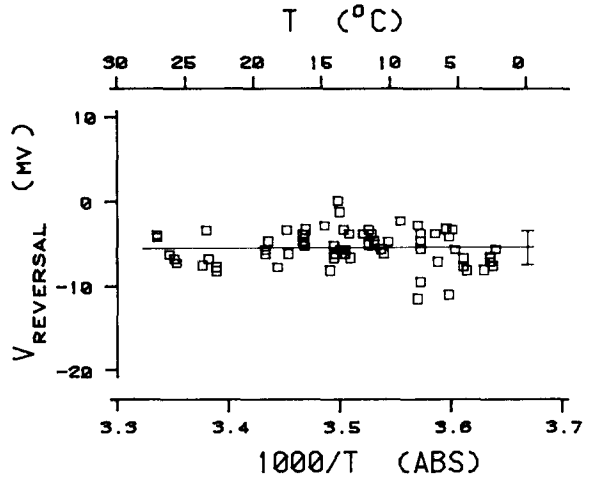

FIGURE 3. Temperature independence of the reversal potential in normal Na saline. 70 measurements, recorded between 1.8 and 26.6°C, are plotted against the reciprocal absolute temperature. A straight line was drawn at the mean reversal potential, −5.60 ± 2.09 mV (mean ± SD).

equations that follow, the expressions for conductance will specify the ions that carry net current. Thus, $\gamma(X)$ is used for the 50%-substituted salines containing Na^+ and ion X^+, and $\gamma(O)$ for normal Na saline.

The slope of the Arrhenius plot was computed by differentiating the natural logarithm of γ with respect to $1/T$, noting that the free-energy terms depend explicitly upon T through the thermodynamic relation

$$\Delta U = \Delta H - T\Delta S. \quad (2)$$

Here ΔH expresses the change in enthalpy and ΔS the change in entropy that accompany the free-energy change at temperature T. When no foreign cations were present in the bath, the slope was given by

$$\frac{\partial \ln[\gamma(O)]}{\partial(1/T)} = -\frac{F\delta V}{R} - \frac{\Delta H_O}{R}, \quad (3)$$

and when equal amounts of Na^+ and cation X^+ were present

$$\frac{\partial \ln[\gamma(X)]}{\partial(1/T)} = -\frac{F\delta V}{R} - \frac{\Delta Ho + \Delta Hx \exp[(\Delta Uo - \Delta Ux)/RT]}{R\{1 + \exp[(\Delta Uo - \Delta Ux)/RT]\}}. \quad (4)$$

These two equations describe the temperature dependence of conductance

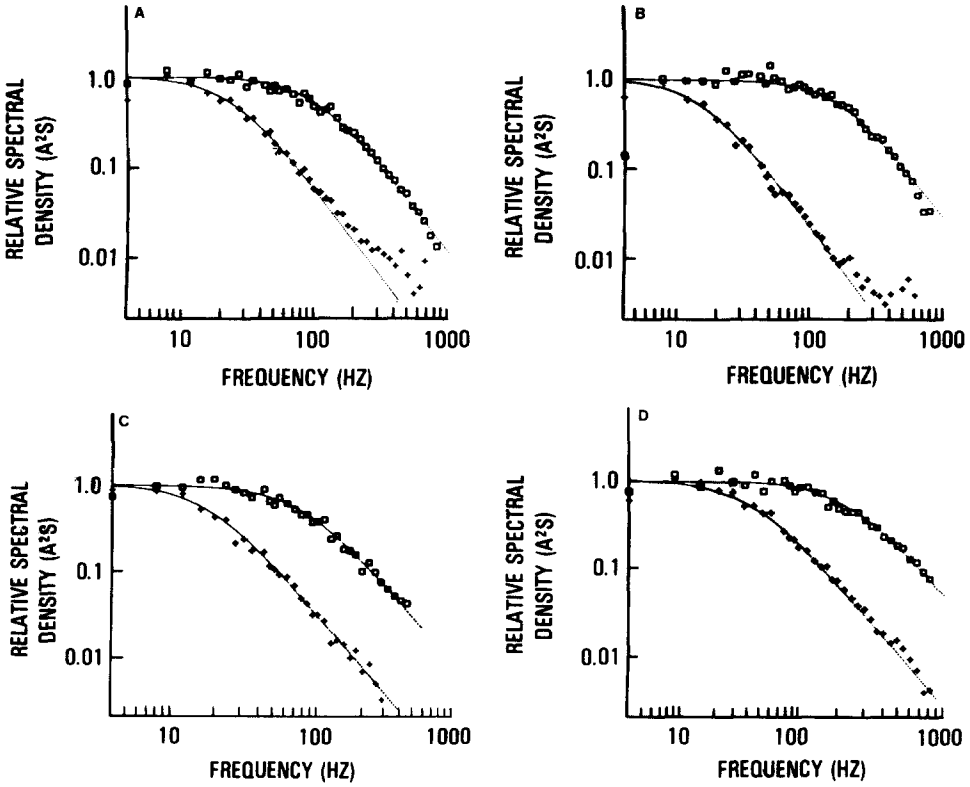

FIGURE 4. Temperature independence of spectral shape. Spectra at all temperatures and in all four solutions were fitted by a single Lorentzian curve. Each of these panels shows two normalized spectra recorded from the same cell at two temperatures. (A) Li was substituted. Two spectra were recorded at 3.0 and 18.4°C; the fitted conductances were 11.1 and 35.7 pS, respectively. The deviation between data and theory at higher frequencies that appears on the lower record is a digitization artifact. (B) Normal Na. Two spectra, recorded at 3.6 and 22.0°C, gave single-channel conductance estimates of 12.8 and 54.1 pS, respectively. (C) Rb was substituted. Two spectra, recorded at 3.0 and 13.6°C, gave conductance estimates of 21.9 and 45.7 pS, respectively. (D) Cs was substituted. Two spectra, recorded at 5.4 and 21.2°C, gave conductance estimates of 38.6 and 103 pS, respectively.

according to the 1B model. In addition, the ion-related differences in magnitude of single-channel conductance should also follow from the net flux equation, but because the vibration frequency was not known, this equation did not provide a useful quantitative description. Instead, we examined

relative changes by evaluating the ratios of conductances measured when foreign cations were present relative to the conductance in normal Na^+ saline. From Eq. 1, with the vibration frequencies of all the alkali metal cations set equal, this conductance ratio can be expressed as

$$\frac{\gamma(X)}{\gamma(O)} = \frac{1}{2}\{1 + \exp[(\Delta U_O - \Delta U_X)/RT]\}. \quad (5)$$

The measured conductance ratio was used with Eq. 5 at a nominal temperature of 10°C to evaluate $(\Delta U_X - \Delta U_O)$, the barrier free-energy difference seen by ion X^+ relative to that for Na^+. In turn, these values were used in the slope equations to evaluate the transfer enthalpy of each permeant cation. For these calculations the barrier was assumed to be symmetric and centrally located in the membrane electric field. Estimates derived from the 1B model are given in Table II and plotted in Fig. 5.

TABLE II

THERMODYNAMIC PARAMETERS ESTIMATED FROM THE SINGLE-BARRIER MODEL

Ion	R	ΔH_X	$\Delta U_X - \Delta U_O$	Q_{10}
	Å	*kcal/mol*	*kcal/mol*	
Li	0.60	9.04±0.65	0.50±0.09	1.88±0.11
Na	0.95	11.44±0.16	0.00±0.05	1.97±0.14
Rb	1.48	11.03±0.44	−0.19±0.05	1.94±0.17
Cs	1.69	11.82±0.34	−0.53±0.05	2.01±0.18

These estimates were obtained by fitting the 1B model to the conductance measurements as outlined in the text. R is the crystal radius, ΔH is the enthalpic height of the barrier, and $\Delta U_X - \Delta U_O$ is the free-energy change seen by ion X relative to Na. All errors are mean ± SE except for the Q_{10}, which is mean ± SD. Estimates were obtained with the barrier positioned at the center of the electric field gradient (δ = 0.5); variation of this parameter between 0 and 1 caused only minor changes in the estimates and did not alter the conclusions.

The 1B model could account for the slopes of the Arrhenius plots and separately for the mean conductances measured in the four test solutions. The slopes were not statistically different (Fig. 5B), with a mean value of −5,155°K, which corresponds to an apparent transfer enthalpy of ~11 kcal/mol. That is, approximately this quantity of heat energy would be necessary for normal ion permeation through the open channel to occur. In contrast, the differences in mean γ that were observed indicate that the transfer free energy for the four permeant cations is graded, according to the 1B model, $\Delta U_{Li} > \Delta U_{Na} > \Delta U_{Rb} > \Delta U_{Cs}$ (Fig. 5C).

In spite of the relative simplicity of the 1B model and the ease of applying it to obtain estimates of the thermodynamic parameters of permeation, the model cannot be correct. The problems are that it does not form a consistent picture when these results are taken together and that it does not describe other published data. Consider these results first. If the transfer enthalpy of the four permeant ions is the same but there are differences in the transfer free energy (above), then there must be differences in the transfer entropies. From

Eq. 2 it follows that the entropic changes that accompany permeation must be graded $\Delta S_{Li} < \Delta S_{Na} < \Delta S_{Rb} < \Delta S_{Cs}$. This indicates an overall change in the coordination among the permeant ion, its hydration waters, and the channel. That is, the hydrated ion must interact with the channel during permeation, and the degree of interaction must differ for the four ions studied. Presumably

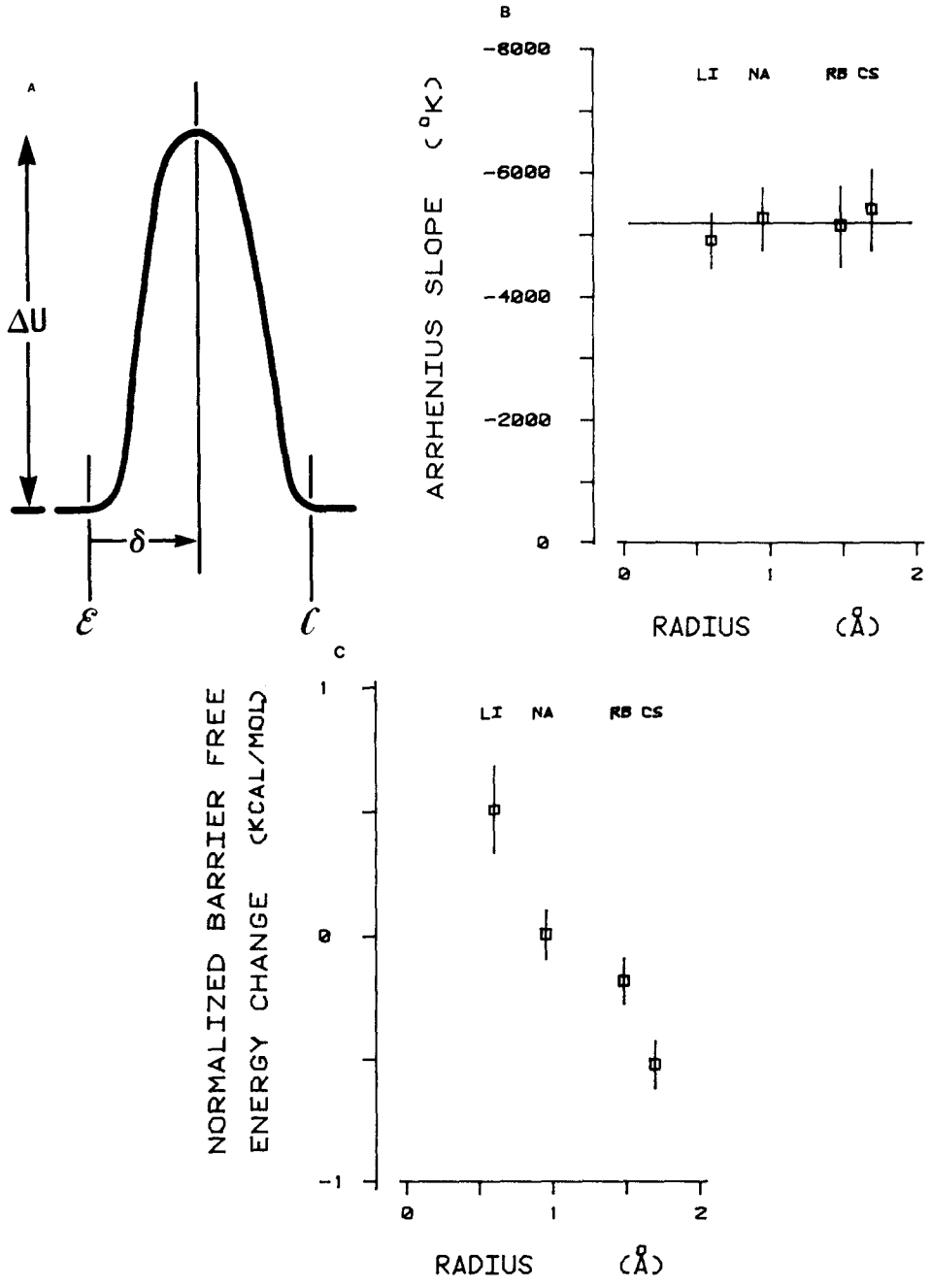

the interaction may be represented as a transient or weak binding phenomenon; however, such a binding process is not explicitly accounted for by the single-barrier model. Furthermore, the permeation studies by Gage and Van Helden (1978), Lewis (1979), Lewis and Stevens (1979), Marchais and Marty (1979), Horn and Patlak (1980), and Adams et al. (1981) all suggest that some degree of binding between the ion and the channel occurs during permeation, and that different permeant ions have different apparent affinities for the channel. Therefore, in order to account for binding, at least one energy well must be postulated together with the energy barrier. That is, the single-barrier model, which has been used to obtain these estimates of the transfer enthalpy and free-energy changes, can only be considered an approximation.

Thus, we have fit our data to a one-barrier/one-site model with the site located on the extracellular side of the barrier (Fig. 6A). The fit is not unique because the number of adjustable parameters in this simple model is large. However, we have tried to introduce what appear to be reasonable constraints for several variables. As shown below, these lead to an enthalpic change between the well bottom and the barrier top of approximately the same amount (~11 kcal/mol) for the four alkali metal ions studied and a shallow well whose depth is graded according to the conductance sequence: Cs > Rb > Na > Li. It appears that the ions that pass through the channel most readily sense a deeper well and so must bind with greater affinity in the channel.

The quantitative relations for the 1B1S model were developed in the same manner as those for the 1B model. They were derived from an expression for the net ionic current that contained separate terms for each permeant ionic species. These ion-specific current terms were expressed as fractions of the transition rates into and out of the well and the transition rates over the barrier (see Lewis and Stevens, 1979). As before, it was through the transition rates that the temperature dependence of permeation was introduced by using the Eyring formalism. Following the procedure outlined above, we expressed the slope of the Arrhenius plot in normal Na saline as

$$\frac{\partial \ln[\gamma(O)]}{\partial(1/T)} = -\frac{F(1-\delta)V}{2R} - \frac{\Delta H_O + \Delta A_O}{R}, \tag{6}$$

FIGURE 5. (*opposite*) Thermodynamic parameters obtained by fitting the single-barrier model to the conductance data. (A) Schematic of the single-barrier model. Free energy is plotted against the reaction distance, which is shown here symmetrically distributed on the membrane. *E* and *C* label the extracytoplasmic and cytoplasmic membrane faces. (B) Ionic independence of the Arrhenius plot slopes. The slopes from Figs. 1 and 2 were arrayed against the crystal radii of the substituted cations. The data indicate no significant dependence on conductance. (C) The mean conductance at 10°C was used to evaluate the relative differences in transfer free energy that accompany the permeant ions (see text). The transfer free energies plotted here for the four permeant cations have been normalized to that of Na. At these temperatures the absolute transfer free-energy values should be close to the enthalpy changes associated with permeation, that is, ~11 kcal/mol. (Both B and C are mean ± 2 SE.)

where ΔH and ΔA are the enthalpic changes of the barrier and the well, respectively, and δ is the relative position of the well in the membrane electric field (Fig. 6A). The expression for the slope in 50%-substituted salines is

$$\frac{\partial \ln[\gamma(X)]}{\partial(1/T)} = -\frac{F(1-\delta)V}{2R} - \frac{\Delta H_O + \Delta H_X \exp[(\Delta U_O - \Delta U_X)/RT]}{R\{1 + \exp[(\Delta U_O - \Delta U_X)/RT]\}} - \frac{\Delta A_O + \Delta A_X \exp[(\Delta E_X - \Delta E_O)/RT]}{R\{1 + \exp[(\Delta E_X - \Delta E_O)/RT]\}}, \quad (7)$$

where ΔU and ΔE are the free-energy changes of the barrier and the well relative to free solution. Finally, the ratio of single-channel conductances can be expressed as

$$\frac{\gamma(X)}{\gamma(O)} = \frac{1 + \exp[(\Delta U_O - \Delta U_X)/RT]}{1 + \exp[(\Delta E_X - \Delta E_O)/RT]}. \quad (8)$$

These three equations (6, 7, 8) contain explicitly the following thermodynamic variables: ΔH_O, ΔH_X, $(\Delta U_O - \Delta U_X)$, ΔA_O, ΔA_X, $(\Delta E_O - \Delta E_X)$, and δ. For this study, using three foreign cations, X^+ in addition to Na^+, these represent a total of 15 variables; however, we have only seven measured parameters: four Arrhenius plot slopes and three conductance ratios. To restrain several variables we have reasoned as follows.

The physical properties of the permeant ions, together with the temperature dependence of ion conductance, suggest that we consider the features in the 1B1S model separately. Consider first the binding interactions between ion and channel. One might expect the different alkali metal cations to exhibit different affinities for the channel because the binding interaction must reflect the electrochemical properties of the ion. The alkali metal cations express a sequence of properties that is graded with ion size; as the crystal radius increases from Li to Cs, the charge density is reduced ~20-fold, hydration number decreases 3–4-fold, and the magnitudes of the solvation energies in both aqueous and nonaqueous solvents decrease ~2-fold (Burgess, 1978). Thus, different species of permeant ions could sense energy wells of various depths. Next, consider the second feature of the 1B1S model, the barrier. Our data suggest that the enthalpy change between the well bottom and the barrier top is relatively insensitive to the specific metal cation. This follows because the Arrhenius plot slope, which is given in Eq. 7 as a weighted sum of barrier and well enthalpy changes accompanying the different permeant ions, appeared to be independent of the specific ions. Thus, we propose that the temperature dependence and conductance of the alkali metal cations must be accounted for by a model that differs mainly in its binding properties and not in the barrier height.

Although such a qualitative argument admits a moderate continuum of values for the parameters in question, consider the extreme case where barrier energies are the same for different ionic species while the binding site energies retain ionic specificity. If we equate the barrier enthalpy, ΔH_O to ΔH_X, and the free energy, ΔU_O to ΔU_X, in the equation for the Arrhenius slopes, these

expressions simplify considerably. It follows that the observation of similar slopes with the different test ions implies that the enthalpy change provided by the well is equal for the permeant ions ($\Delta A_O = \Delta A_X$). This is consistent with the qualitative argument above that the enthalpy change between the

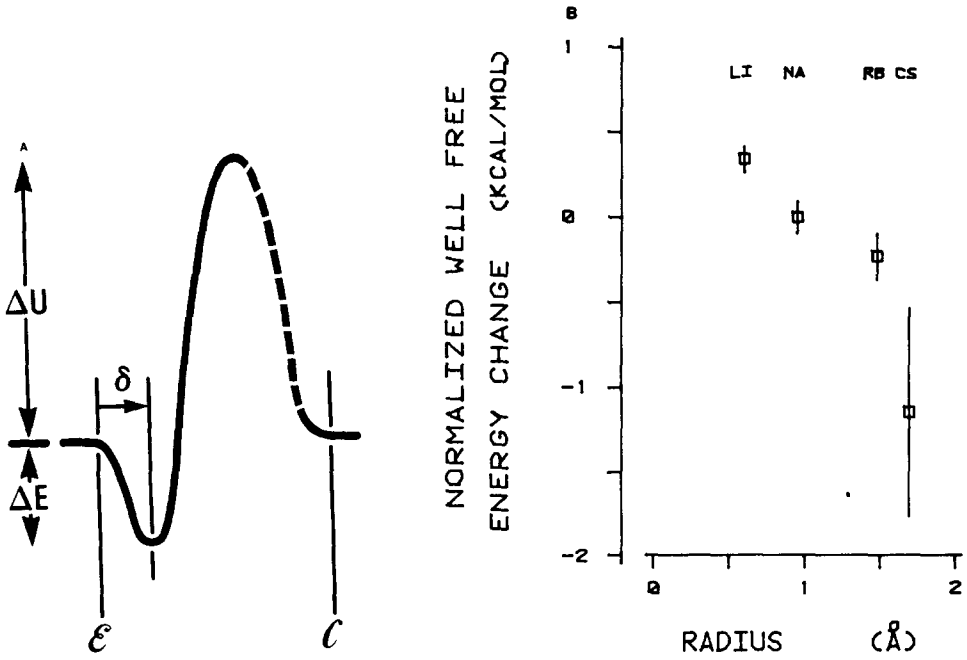

FIGURE 6. Thermodynamic parameters obtained by fitting the 1B1S model to the conductance data. (A) Schematic of the 1B1S model. Free energy is plotted against the reaction coordinate. The barrier free energy, ΔU, and well depth, ΔE, are shown relative to the solution level. E and C label the extracytoplasmic and cytoplasmic faces of the membrane, respectively. The portion of the energy profile facing the cytoplasmic side (C face) has been drawn as a dashed line because these data, which result from inward directed currents, give little information on that part of the curve. (B) Ionic dependence of the binding site free energy. The relative binding site free energy was evaluated with Eq. 9 and is plotted here against the crystal radii of the permeant ions. These energies are relative to that experienced by Na when it binds at the site. Fitting the 1B1S model to these data did not allow an estimate of the absolute free-energy depth of the well for any ion; however, given the overall rate of ion permeation, the 11.23 kcal/mol enthalpy change from the well bottom to the barrier top, and the expected similarity of enthalpy and free-energy values at the working temperatures, the actual well depths are probably on the order of 2–6 kcal/mol.

well bottom and the barrier top is approximately the same for the four ions examined. For this case the estimate of that enthalpy change is 11.23 ± 0.16 kcal/mol (mean ± SE). The relative well free-energy difference between ions ($\Delta E_X - \Delta E_O$) can be calculated from the conductance ratio, which is simplified

by this approximation to

$$\frac{\gamma(X)}{\gamma(O)} = \frac{2}{1 + \exp[(\Delta E_X - \Delta E_O)/RT]}. \quad (9)$$

Estimates for the relative free-energy difference were obtained by fitting Eq. 9 to the data; they appear in Table III and are plotted in Fig. 6B.

Thus we have a picture of inward-directed ion permeation through the AChR channel. The cations must first bind at a site in the mouth of the channel and from there pass through an energetically less favorable region of the channel lumen to reach the cytoplasm. This second step can be accomplished only if the ions acquire sufficient kinetic energy. This energy is taken from the microscopic environment in discreet amounts via thermally driven collisions with neighboring ions, atoms, and molecules. These collisions, which occur with a frequency on the order of 10^{11}/s, transfer energy in amounts

TABLE III

THERMODYNAMIC PARAMETERS ESTIMATED FROM THE ONE-BARRIER/ONE-SITE MODEL

Ion	R	$\Delta H_X + \Delta A_X$	$\Delta E_X - \Delta E_O$	$\Delta S_X - \Delta S_O$
	Å	*kcal/mol*	*kcal/mol*	*cal/mol °K*
Li	0.60	11.23±0.16	0.34±0.04	−1.20±0.14
Na	0.95	11.23±0.16	0.00±0.05	0.00±0.18
Rb	1.48	11.23±0.16	−0.23±0.07	0.81±0.25
Cs	1.69	11.23±0.16	−1.15±0.31	4.06±1.10

These estimates were obtained by fitting the 1B1S model to the conductance measurements as outlined in the text. R is the crystal radius, $\Delta H_X + \Delta A_X$ is the enthalpic height of the barrier measured from the well bottom, $\Delta E_X - \Delta E$ is the free-energy depth of the well for ion X relative to that for Na, and $\Delta S_X - \Delta S_O$ is the entropy change that occurs when ion X binds in the well relative to that for Na. These estimates were obtained with the well positioned 20% through the membrane electric field ($\delta = 0.2$). All errors are means ± SE.

having a Boltzmann distribution; very small amounts will be exchanged often while the frequency of acquiring increasingly large quantities of energy will be exponentially smaller. Then the likelihood that any ion successfully permeates the membrane will depend in part upon the length of time it spends bound to the site, since this will increase the number of energy exchange interactions it experiences. This bound sojourn is terminated when the ion acquires enough energy to leave the site; either it crosses the barrier or it is kicked back into the extracellular milieu. Thus, permeation is a competitive process where an ion enters the well and takes a chance on its future. If it collects enough kinetic energy to pass through the channel before it is kicked back out, it can penetrate the membrane. However, when the barrier to permeation is far greater than the energy needed to back out of the well, the ion has only a small chance of permeating.

Within this framework, an increase in affinity of the ion for the channel can result in a larger permeability for the ion. In effect, this occurs because the

more tightly bound ions are less likely to be dislodged from the channel by the small thermal perturbations that prevail; this augments the probability that these ions will be present at the site when an energetic collision occurs, enabling the ion to cross the barrier. For a well depth in the range of 1–6 kcal/mol and a barrier height (measured from the well bottom) of 11 kcal/mol, an increment in well depth of 1 kcal/mol will cause an increased conductance of nearly threefold. Thus, the relative conductance of different ions may be determined not by the frequency with which they gain access to the channel or by the height of the energy barrier to permeation but by the affinity with which they bind within the channel.

This model postulates a site at which permeant ions bind before they can cross the membrane. Thus, competition among permeant ions must occur and the independence principle should not hold for the AChR channel. Indeed, Adams et al. (1981) have obtained evidence for the AChR channel that permeant organic ions at normal concentrations do not behave according to the independence principle, although the small monovalent cations show little deviation. At higher concentrations, Na ions, also, show saturation (Horn and Patlak, 1980). We believe that competition among permeant ions for a site in the channel occurs generally, although under the conditions of these experiments its effects were minimal and not specifically considered in our models. At normal ion concentrations the apparent adherence to the independence principle by the alkali metal cations may reflect a brief residency time for these ions at the site. Therefore, the saturation effects that show up as violations of the independence principle should not have been observed.

It might be noted that affinity changes between the channel and the ion could also account for channel gating. That is, when an ion binds very weakly to the channel, it has virtually no chance of successfully crossing the membrane since the smallest bit of thermal energy can expel it. For such ions, the channel appears effectively closed. In principle, then, a deceptively simple but effective gating mechanism could be produced for the AChR channel if the well depth were modulated by the binding of agonist molecules. The major difference between this mechanism and the "trap-door"-like mechanisms often imagined is that little physical restructuring of the protein need accompany the gating action and activation would be consistent with the observation that the channel opening rate shows little voltage sensitivity (Dionne and Stevens, 1975). Indeed, the channel lumen could be structurally open at all times whether it was gated "open" or "closed" for ion permeation. It might be possible to distinguish experimentally between these two types of gating mechanisms by examining the flux of a neutral molecular probe. The only published data on nonelectrolyte fluxes through the AChR channel (Huang et al., 1978) provides no test between these mechanisms because of the type of controls that were used.

One additional implication of this description is that the ion-specific fraction of the binding process between ion and channel is an entropic interaction in which the channel must substitute for the environment provided by water molecules to a small degree. However, we do not believe that the channel

replaces the entire hydration shell of the permeant ions because that would require a comparatively large energy (Burgess, 1978). Thus, we suspect that the ions that pass through the channel move with their hydration shells virtually intact. Finally, the model does not account for the nonlinear and discontinuous Arrhenius plots that have been described by others (see the Introduction). It is plausible, however, that lipid-protein interactions or a temperature-dependent change in the structure of the binding site or barrier could account for those results.

Although this description of ion permeation is not a unique model of these data, it is both simple and consistent with our evidence on relative conductance and ion interaction with the channel. Note, in addition, that a single binding site for ions on the extracellular side of the barrier does not exclude the presence of additional binding on the cytoplasmic side of the channel. Since our measurements were made under conditions where the net flux of ions through the channel was almost entirely equal to the inward-directed one-way flux, one or more shallow intracellular energy wells would not have affected the single-channel currents. Indeed, we might expect such sites to exist, and Adams et al. (1981) have obtained evidence for binding of ions at a site that is readily accessible from the inside of the channel.

Supported by National Institutes of Heath grant NS 15344.

Received for publication 28 October 1982 and in revised form 20 December 1982.

REFERENCES

Adams, D. J., T. M. Dwyer, and B. Hille. 1980. The permeability of endplate channels to monovalent and divalent metal cations. *J. Gen. Physiol.* 75:493–510.

Adams, D. J., W. Nonner, T. M. Dwyer, and B. Hille. 1981. Block of endplate channels by permeant cations in frog skeletal muscle. *J. Gen. Physiol.* 78:593–615.

Anderson, C. R., S. G. Cull-Candy, and R. Miledi. 1977. Potential-dependent transition temperature of ionic channels induced by glutamate in locust muscle. *Nature (Lond.).* 268:663–665.

Anderson, C. R., and C. F. Stevens. 1973. Voltage clamp analysis of acetylcholine produced end-plate current fluctuations at frog neuromuscular junction. *J. Physiol. (Lond.).* 235:655–691.

Ascher, P., A. Marty, and T. O. Neild. 1978. Lifetime and elementary conductance of the channels mediating the excitatory effects of acetylcholine in *Aplysia* neurones. *J. Physiol. (Lond.).* 278:117–206.

Burden, S. J., H. C. Hartzell, and D. Yoshikami. 1975. Acetylcholine receptors at neuromuscular synapses: phylogenetic differences detected by snake alphaneurotoxins. *Proc. Natl. Acad. Sci. USA.* 72:3245–3249.

Burgess, J. 1978. Metal Ions in Solution. Ellis Horwood, Ltd. 481 pp.

Dionne, V. E. 1981. The kinetics of slow muscle acetylcholine-operated channels in the garter snake. *J. Physiol. (Lond.).* 310:159–190.

Dionne, V. E., and R. L. Parsons. 1981. Characteristics of the acetylcholine-operated channel in twitch and slow fiber neuromuscular junctions of the garter snake. *J. Physiol. (Lond.).* 310:145–158.

Dionne, V. E., and M. D. Leibowitz. 1982. Acetylcholine receptor kinetics: a description from single-channel currents at snake neuromuscular junctions. *Biophys. J.* 39:253–261.

Dionne, V. E., and C. F. Stevens. 1975. Voltage dependence of agonist effectiveness at the frog neuromuscular junction: resolution of a paradox. *J. Physiol. (Lond.).* 251:245–270.

Dreyer, F., K. D. Müller, K. Peper, and R. Sterz. 1976. The m. omohyoideus of the mouse as a convenient mammalian muscle preparation. *Pflügers Arch. Eur. J. Physiol.* 367:115–122.

Fischbach, G. D., and Y. Lass. 1978. A transition temperature for acetylcholine channel conductance in chick myoballs. *J. Physiol. (Lond.).* 280:527–536.

Gage, P. W., and D. Van Helden. 1979. Effects of permeant monovalent cations on end-plate channels. *J. Physiol. (Lond.).* 288:509–528.

Hartzell, H., S. W. Kuffler, and D. Yoshikami. 1975. Post-synaptic potentiation: interaction between quanta of acetylcholine at the skeletal neuromuscular synapse. *J. Physiol. (Lond.).* 251:427–463.

Horn, R., and J. Patlak. 1980. Single channel currents from excised patches of muscle membrane. *Proc. Natl. Acad. Sci. USA.* 77:6930–6934.

Huang, M. L.-Y., W. A. Catterall, and G. Ehernstein. 1978. Selectivity of cations and nonelectrolytes for acetylcholine-activated channels in cultured muscle cells. *J. Gen. Physiol.* 71:397–410.

Kuffler, S. W., and D. Yoshikami. 1975. The number of transmitter molecules in a quantum: an estimate from iontophoretic application of acetylcholine at the neuromuscular synapse. *J. Physiol. (Lond.).* 251:465–482.

Lass, Y., and G. D. Fischbach. 1976. A discontinuous relationship between the acetylcholine-activated channel conductance and temperature. *Nature (Lond.).* 263:150–151.

Lewis, C. A. 1979. Ion-concentration dependence of the reversal potential and the single channel conductance of ion channels at the frog neuromuscular junction. *J. Physiol. (Lond.).* 286:417–445.

Lewis, C. A., and C. F. Stevens. 1979. Mechanism of ion permeation through channels in a postsynaptic membrane. *In* Membrane Transport Processes. C. F. Stevens and R. W. Tsien, editors. Raven Press, New York. 133–151.

Marchais, D., and A. Marty. 1979. Interaction of permeant ions with channels activated by acetylcholine in *Aplysia* neurones. *J. Physiol. (Lond.).* 297:9–45.

Nelson, D. J., and F. Sachs. 1979. Single ionic channels observed in tissue-cultured muscle. *Nature (Lond.).* 282:861–863.

Sachs, F., and H. Lecar. 1977. Acetylcholine-induced current fluctuations in tissue-cultured muscle cells under voltage clamp. *Biophys. J.* 17:129–143.